

## Original Article

# New Hosts and Comparison of Biological and Molecular Characteristics of Fig, Mulberry, and Citrus Isolates of Hop Stunt Viroid in Iran

Jahanshahi Z , Izadpanah K\* , Afsharifar AR, Behjatnia SAA

Plant Virology Research Center, College of Agriculture, Shiraz University, Shiraz, Iran

### Abstract

**Background and Aims:** Hop stunt viroid (HSVd, genus Hostuviroid, family Pospiviroidae) has a wide host range among trees and herbaceous plants. The objectives of this study were to compare biological and physical characteristics of three isolates of HSVd from mulberry, fig and citrus and search for other hosts of this viroid in Iran.

**Materials and Methods:** Plant samples were collected from Yazd, Isfahan, Fars and Tehran provinces and examined for their possible infection by hop stunt viroid (HSVd) using reverse transcription- polymerase chain reaction (RT-PCR). The experimental host range of the viroid was determined by injection of infected sap into greenhouse grown seedlings and subsequent assay of inoculated plants by RT-PCR. Fig, mulberry and citrus isolates of the viroid were compared with respect to host range and molecular characteristics. Nucleic acids were isolated from plant tissues by CTAB method and subjected to RT-PCR using HSVd specific primers. The PCR products were sequenced and the most stable secondary structures for the three mentioned isolates were predicted and compared.

**Results:** Among 120 samples collected from different regions and hosts, 13 samples from mulberry, fig, apple, quince, apricot, peach and citrus were infected by HSVd. The mulberry samples showed vein clearing and leaf deformation symptoms while usually no specific symptoms were observed in the fig samples. Apple, quince, apricot, peach and citrus samples were also symptomless hosts. In greenhouse tests, mulberry isolate induced more severe symptoms. Comparison of primary and secondary structures of the viroid isolates showed a closer similarity between the fig and mulberry isolates while the latter were less similar to citrus isolate.

**Conclusions:** Sequence variation and structural differences were observed among the isolates studied. Most differences of these isolates were in the pathogenicity, variable and terminal right regions which may determine the type and severity of symptoms. Many trees are infected without showing apparent symptoms.

**Keywords:** hop stunt viroid, fig, citrus, mulberry

### Introduction

Viroids are naked, small, single-stranded RNA molecules of 246–401 nucleotides (1). They replicate

\*Corresponding author: Keramtollah Izadpanah. Plant Virology Research Center, College of Agriculture, Shiraz University, Shiraz, Iran. Email: izadpana@shirazu.ac.ir

autonomously in host plants and may cause diseases or latent infections (2). Hop stunt viroid (HSVd, genus *Hostuviroid*, family *Pospiviroidae*) has a wide host range, infecting herbaceous crops and many fruit tree species (Hadidi et al., 2003). In most hosts, including grapevine (3, 4) and apricot (5), HSVd infection appears to be latent. In other cases, HSVd infection has been associated with specific disorders such as hop stunt (3), dapple fruit of plum and peach (6) and citrus cachexia (7, 8). Overall, sequence homologies (3) and phylogenetic analyses (9) indicate that HSVd isolates can be separated into three major groups and two sub-groups which are apparently resulted from recombination between members of the major groups (10). The major groups were named plum-type (peach, plum and grapevine isolates), hop-type (hop, grapevine, peach and pear isolates) and citrus-type (citrus and cucumber isolates). In Iran, HSVd has been isolated from a number of crop plants including citrus, fig and mulberry (11, 12, 13). The purpose of this study was to compare biological and molecular features of these isolates and to explore possible infection of other plants by HSVd.

### Methods

**Sampling.** In summer of 2013, 120 plant samples were collected in Fars (Estahban, Kazeroun, Sepidan and Shiraz), Yazd, Isfahan, Boushehr (Borazjan), and Tehran provinces from fig, citrus, mulberry and a number of other plant species. The samples were either symptomless or showed vein clearing, leaf deformation or yellowing.

**Mechanical inoculation of herbaceous test plants.** The mulberry (HSVd-Bor), citrus (HSVd-F2) and fig (HSVd-F3) isolates of HSVd from Borazjan (Boushehr province), Shiraz (Fars province), and Estahban (Fars province) were inoculated to herbaceous plants by injection of infected sap into greenhouse grown seedlings of *Cucumis sativus*, *Cucumis melo* var *reticulata*, *Citrullus lanatus*, *Nicotiana tabacum* cv *Turkish*, *Gossypium* sp., *Beta vulgaris*, *Spinacia oleracea*, *Phaseolus vulgaris*, *Vigna unguiculata*, *Vigna radiata* and *Solanum*

*lycopersicum*. Inoculated plants were maintained for 4 weeks in the greenhouse, observed for symptom development and subsequently assayed for the presence of HSVd by RT-PCR.

**Nucleic acid extraction.** Total nucleic acid was extracted from leaf vein tissues using the CTAB method described by Gambino et al. (14) with slight modification. Each sample (200 mg) was powdered in liquid nitrogen and mixed with four volumes (800  $\mu$ L) of preheated (65°C) extraction buffer (2% CTAB, 2% PVP-40, 2 M NaCl, 200 mM Tris-HCl, pH 8.0, 1% sodium lauryl sarcosine, 20mM sodium borate and 2%  $\beta$ -mercaptoethanol). The mixture was incubated at 65°C for 10 min and extracted three times with an equal volume of chloroform: isoamyl alcohol (24:1 v/v), an equal volume of phenol: chloroform: isoamyl alcohol (25:24:1 v/v/v) and an equal volume of chloroform: isoamyl alcohol (24:1 v/v), respectively. The nucleic acid extract was incubated with a half volume of 8 M Lithium chloride at 20°C overnight. The nucleic acids were recovered by centrifugation at 15000g for 15min at 4°C. The pellet was washed in 70% ethanol, dried and resuspended in DEPC-treated water.

**Synthesis, amplification and sequencing of the viroid cDNA.** A specific HSVd primer pair (F: 5'-GGC AAC TCT TCT CAG AAT CCA GC-3'/ R: 5'-CCG GGG CTC CTT TCT CAG GTA SGT-3') was used for reverse transcription and amplification of the viroid DNA template. To generate the cDNA from viroid RNA, 2  $\mu$ L of the reverse primer (10  $\mu$ M) was mixed with 5  $\mu$ L of nucleic acid preparation, heated at 70°C for 10 min and chilled on ice immediately. Reverse transcription was carried out in a 20  $\mu$ L reaction volume containing the RNA template and primer, 50 mM Tris-HCl, pH 8.3, 50 mM KCl, 4 mM MgCl<sub>2</sub>, 10 mM dithiothreitol, 1mM each dNTP and 200 units of MMuLV reverse transcriptase (Fermentas, Lithuania). The mixture was incubated at 42°C for 60 min to generate the first strand cDNA. PCR reaction was carried out in 25  $\mu$ L volumes containing 4 $\mu$ L of the first strand cDNA, 1.5 mM MgCl<sub>2</sub>, 200  $\mu$ M of each dNTP, 0.3 $\mu$ M of each primer

and 0.125 U of Taq DNA polymerase (Cinagen, Iran) in the reaction buffer provided by the same source. The mixture was subjected to an initial denaturation step at 94°C for 3 min and 35 cycles of 94°C for 1 min, 60°C for 30 seconds and 72°C for one min. The final cycle was followed by 15 min incubation at 72°C. PCR products were visualized in 1.0 % agarose gel containing 0.5 µg ml<sup>-1</sup> ethidium bromide in TBE buffer. PCR products were purified by an AccuPrep® PCR Purification Kit (BIONEER) according to the manufacturer's instructions and sent to Bioneer (South Korea) for sequencing.

**Sequence analysis.** The nucleotide sequence data of HSVd isolates obtained in this study have been deposited in GenBank (their accession numbers have been mentioned in Results section) and aligned with each other and other viroid sequences deposited in GenBank using BLAST program from the National Center for Biotechnology Information (NCBI). The sequence data were analyzed by Vector NTI version 10.3 and DNASTAR packages and the most stable RNA secondary structures of the HSVd sequences were predicted using the Version 5 of RNA Secondary Structure Prediction package.

## Results

**Hosts and symptoms.** Herbaceous host range of fig, citrus and mulberry isolates of HSVd were almost the same (Table 1) except for infection of spinach (*Spinacia oleracea*) by mulberry isolate (HSVd-Bor) while the other two isolates did not infect this plant. HSVd-Bor induced more severe symptoms in herbaceous hosts compared to milder symptoms induced by two other isolates (Table 1, Fig. 1). It replicated in all test plants (Table 1) and induced severe stunting and yellowing in *Cucumis sativus*, epinasty and yellowing in *Solanum lycopersicum* and leaf curl in *Beta vulgaris*. HSVd-Bor also induced stunting but no other obvious symptoms in *Nicotiana tabacum*.

Among 120 plant samples tested by PCR, 13 samples including fig from Yazd (Acc. No. KP126940) and Estahban (KP126941, 42), mulberry from Shiraz (KP126945 and KP126948), Borazjan (KP126946) and Yazd (KP126947), citrus from Shiraz (KP126951, 52), apple from Sepidan (KP126944), quince from Sepidan (KP126943), peach from Yazd (KP126949), and apricot from Yazd (KP126950) were infected with HSVd. Except for mulberry that showed vein clearing and leaf curling the other HSVd positive samples showed no specific symptoms. All other samples collected from plum, almond, peach, apple, grapevine and pomegranate were PCR negative.

**Molecular and structural analysis of HSVd isolates.** The expected PCR products obtained from different hosts were sequenced. Comparison of the resulting nucleotide sequences with those available in GenBank using BLAST program revealed that these sequences were indeed the sequence variants of HSVd consisting of 301-305 nt in mulberry isolates, 302-304 nt in fig isolates, 300-302 nt in citrus isolates and 296-303 nt in apricot, peach, apple and quince. Comparison of primary structure of fig (F3), mulberry (Bor) and citrus (F2) isolates based on multiple alignment (Figs. 2, 3, 4) showed that HSVd-F3 and HSVd-Bor genomes are closely similar especially in terminal left (TL) and central conserved regions (CCR). The differences between these two isolates were mainly related to the pathogenicity (P) and terminal right (TR) regions. HSVd-F3 and HSVd-Bor were different from HSVd-F2 in all regions. Differences in primary structure between these isolates resulted in considerable changes in their predicted secondary structures (Figs. 2, 3, 4) including the shape, size and number of inner loops and also in free energy of structure formation ( $\Delta G$ ) (Table 2), so that the HSVd-Bor isolate had the lowest while the HSVd-F2 had the highest free energy of structure formation. Furthermore, there are two fewer loops in the HSVd-Bor isolate. On this basis, citrus isolate appears to have the most stable structure.

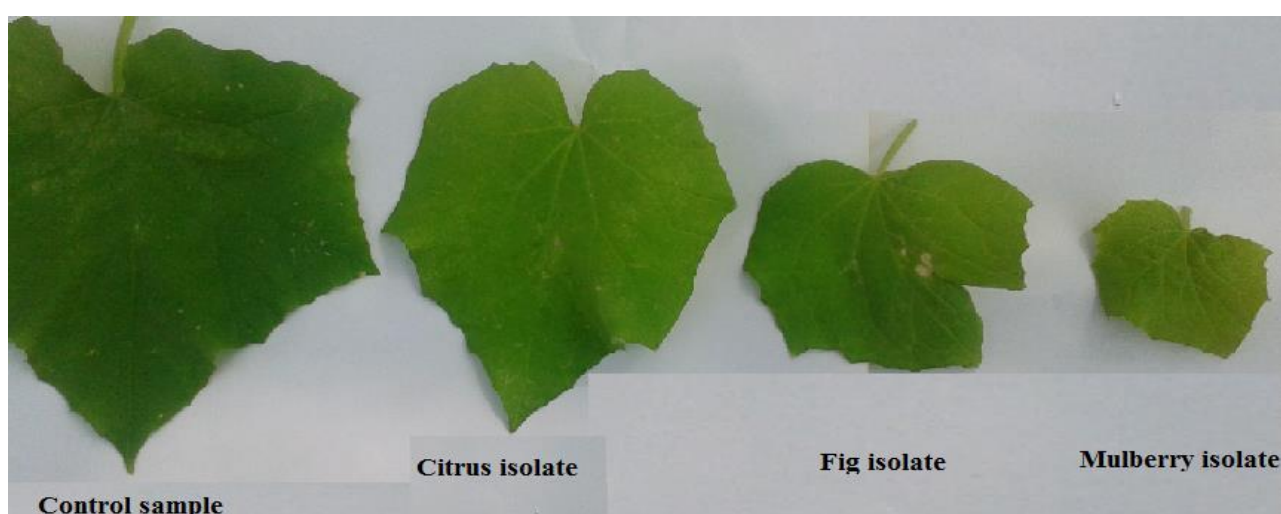


**Fig. 1.** Comparison of symptom severity induced by citrus, fig and mulberry isolates of HSVd on inoculated *Cucumis sativus*. The mulberry isolate induced more severe symptoms.

**Table 1:** Comparison of host range and symptoms of mulberry, fig, and citrus isolates of HSVd under greenhouse conditions

Hosts	Symptoms		
	HSVd-Bor (mulberry)	HSVd-F3 (fig)	HSVd-F2 (citrus)
<i>Cucumis sativus</i>	Yellowing, stunting	Yellowing, stunting	Yellowing, stunting
<i>Cucumis melo</i> var. <i>reticulata</i>	Yellowing, stunting	Yellowing, stunting	None
<i>Nicotiana tabacum</i> cv. Turkish	Stunting,	Stunting	Stunting
<i>Solanum lycopersicum</i>	Epinasty, yellowing, tiny foliage	Yellowing, tiny foliage	Yellowing, tiny foliage
<i>Beta vulgaris</i>	Leaf curl	Leaf curl	Mosaic
<i>Spinacia oleracea</i>	Stunting, mosaic	None	None

**Table 2:** Comparison of free energy ( $\Delta G$ ) and number of inner loops in the secondary structure of mulberry, fig, and citrus isolates of HSVd

Isolate	Number of loops	$\Delta G$ (kcal)
HSVd-Bor (mulberry)	26	-110.7
HSVd-F3 (fig)	28	-112.9
HSVd-F2 (citrus)	28	-119.2

Terminal left region of HSVd genome consists of nucleotides 1-30 in upper strand and 280-305 nucleotides in lower strand (15 with minor variation in different isolates (16)). The same was true with the three Iranian HSVd isolates analyzed in this study. They all had three loops in this region (Fig. 2). HSVd-Bor and HSVd-F3 showed 100% homology in sequence and secondary structure of this region while C25T and A26G changes and A27 deletion were found in HSVd-F2 (Fig. 2). The P region

contains nucleotides 31-60 in the upper strand and 242-278 in the lower strand (15). Molecular comparison of P region in these three isolates (Fig. 2) showed that nucleotide 45 is T in HSVd-Bor and A in HSVd-F3 isolates while T45, C46 and G60 were absent in the genome of HSVd-F2 (Fig. 2). More differences between these three isolates in P region were related to the lower strand, resulting in variation in the number, shape and size of inner loops (Fig 2).

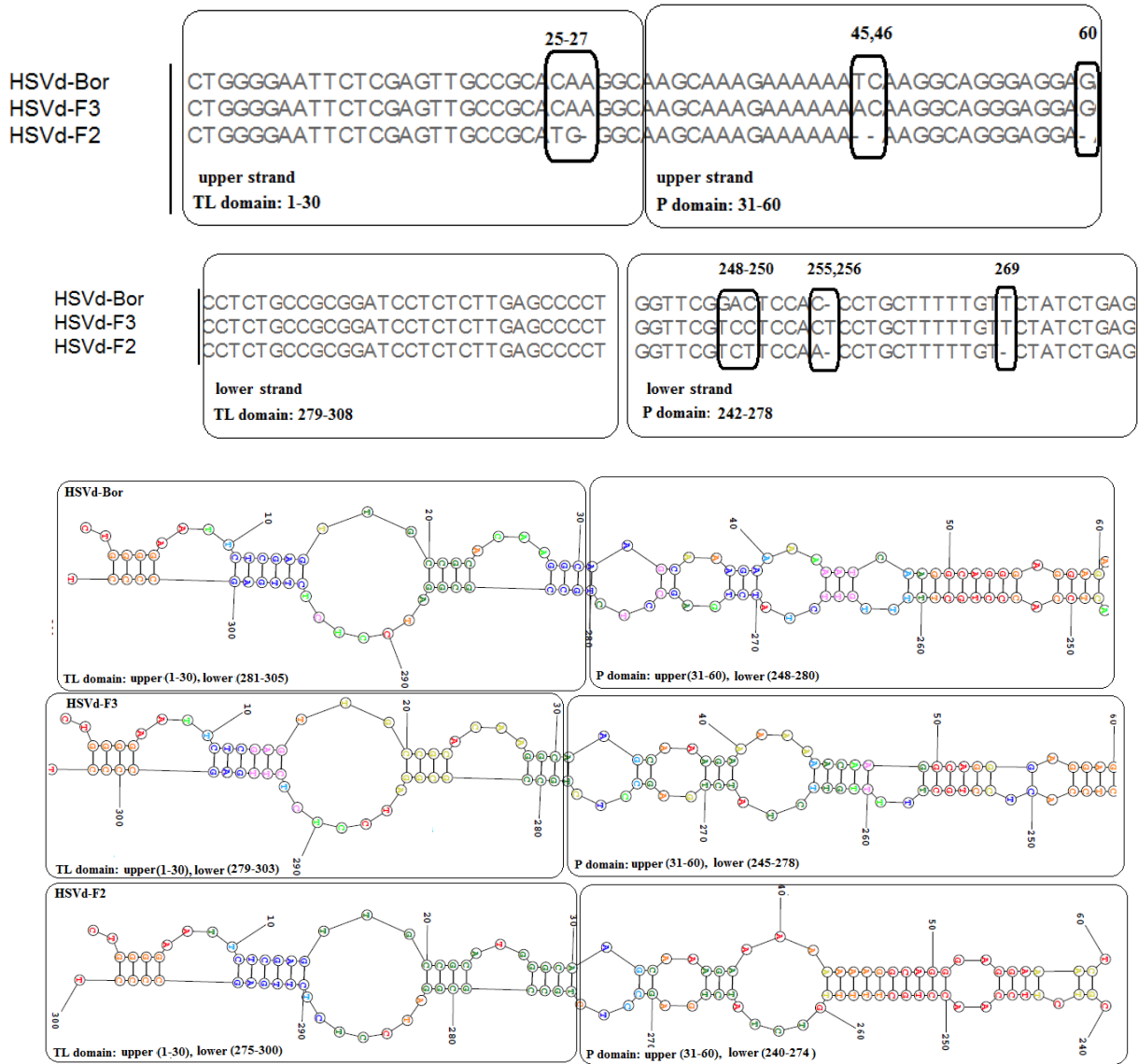


**Fig. 2.** Structure of terminal left (TL) and pathogenicity (P) domain in mulberry (Bor), fig (F3) and citrus (F2) isolates of HSVd. Top, primary structure. Differences are indicated by circles. Bottom, secondary structures of HSVd-Bor, -F3, and -F2 isolates showing various loops in TL and P domain. Increase in the number of nucleotides in lower TL (308 instead of 305) is due to alignment of sequences.

Central conserved region (CCR) contains nucleotides 61-105 in the upper strand and 198-241 in the lower strand (15). The three isolates showed a high rate of homology in the upper strand of CCR (Fig. 3). But the lower strand of this region in HSVd-F2 was quite different from the other isolates affecting the size and shape of the inner loops. Variable (V) region contains nucleotides 106-125 in the upper strand and nucleotides 179-197 in the lower strand (15). Molecular comparison of this region (Fig. 3) showed that A110 in HSVd-F3 genome and A118 in HSVd-Bor and

HSVd-F2 genome are deleted and T117A in HSVd-F2 is changed.

The TR region comprises nucleotides 126-151 in the upper strand and 152-178 in the lower strand (15). Multiple alignment of HSVd-F2, HSVd-Bor and HSVd-F3 genomes (Fig. 4) showed that most differences were located on the upper strand. There were the same numbers of loops although different in size and shape.

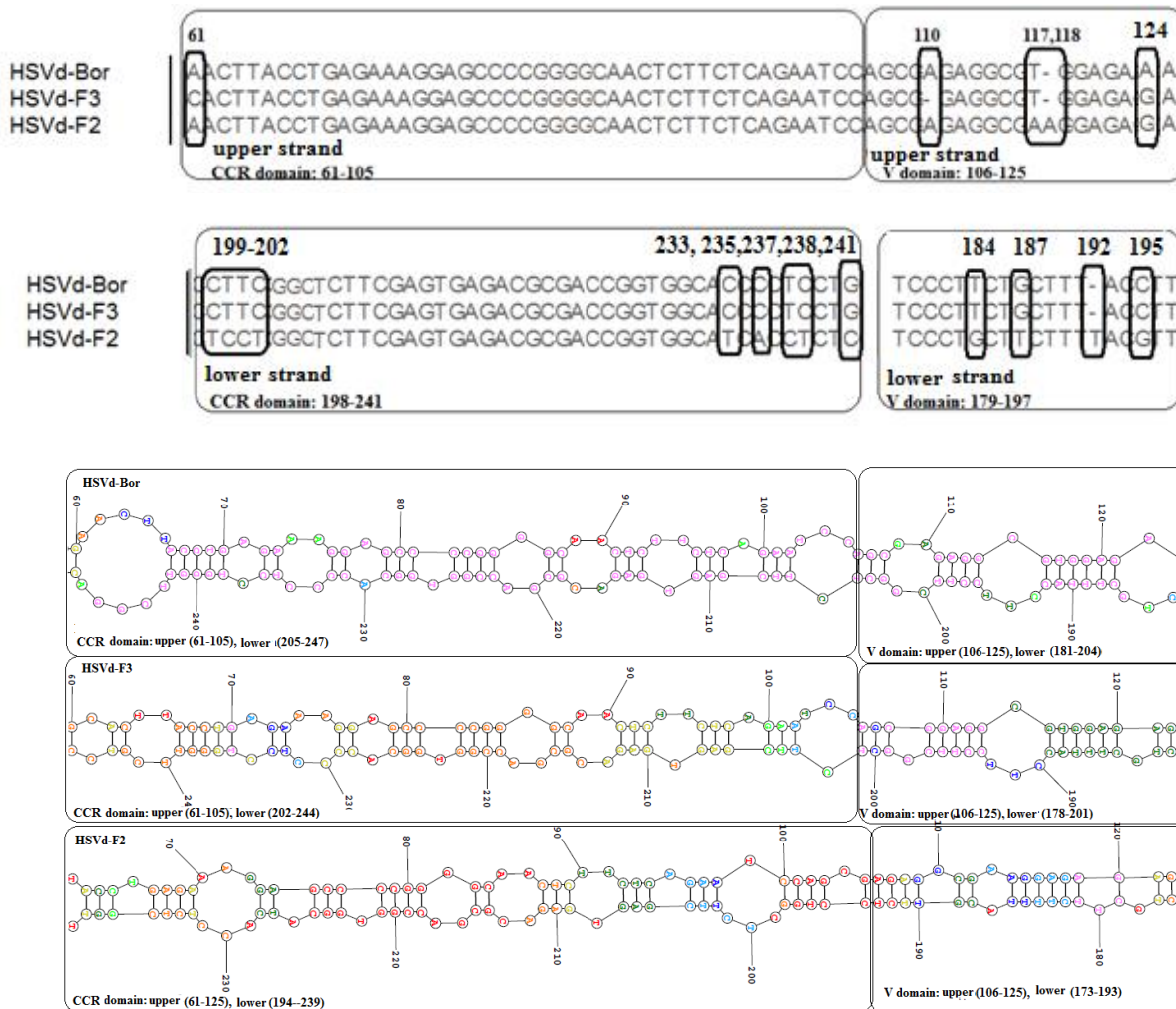


**Fig. 3.** Structure of central conserved (CCR) and variable (V) domain in mulberry (Bor), fig (F3) and citrus (F2) isolates of HSVd. Top, primary structure. Differences are indicated by circles. Bottom, secondary structures of HSVd-Bor, -F3 and -F2 in CCR and V domain. Note differences in the number and size of the loops.

## Discussion

Among viroids, HSVd seems to have the widest natural host range (17). Most variants of this viroid induce no discernable symptoms in the infected plants but some are associated with distinct diseases such as citrus cachexia, hop stunt and mulberry vein clearing (3, 6, 7, 11, 18 ). Differences in the biological characteristics of viroids are due to differences in their nucleotide composition and secondary structure (15, 16, 19, 20, 21, 22, 23, 24, 25, 26 ). In the present study three isolates of HSVd were compared for their host range, symptomology, nucleotide sequence and secondary structure. HSVd-Bor isolate from mulberry exhibited the most severe symptoms. This maybe due to lower free energy of structure formation and lower temperature of

denaturation (21) which may result in increased replication rate and consequently more severe symptoms in herbaceous plants. However, similar stability in the terminal left region of mulberry, citrus and fig isolates showed that possible increase in replication rate of HSVd-Bor isolate in host plants is not determined by this region. The main differences between the genome of these three isolates were observed in the P region which is responsible for controlling pathogenicity and symptom severity (27). P domain also interacts with TL domain in replication (27, 28, 29). The nucleotides 35 to 46 on the upper strand and 264 to 272 on the lower strand have been regarded as the pathogenicity modulating (PM) region while nucleotides 30 to 46 on the upper strand and 264 to 280 on the lower strand have been regarded as the virulence modulating

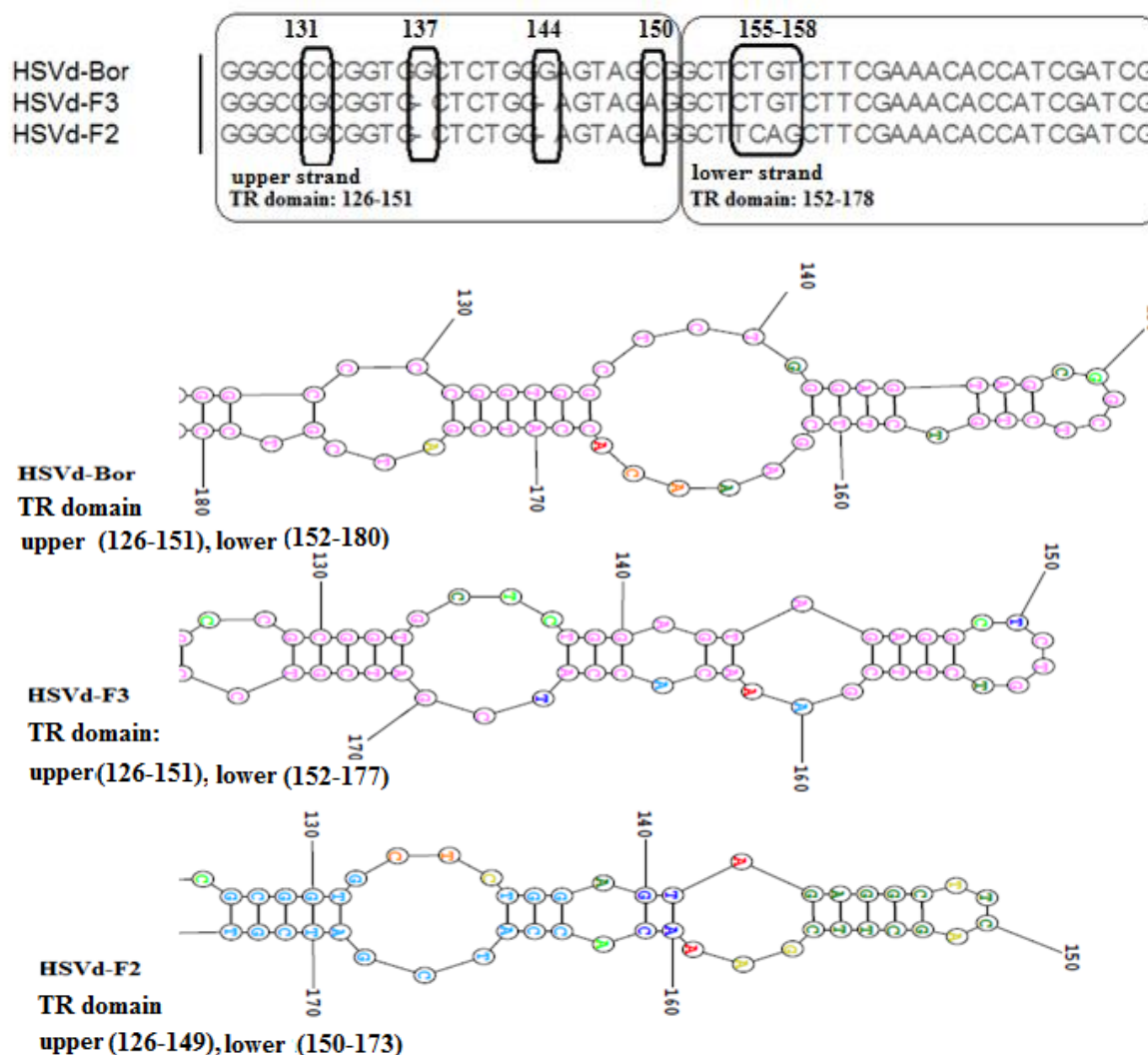


**Fig. 4.** Structure of terminal right (TR) domain in mulberry (Bor), fig (F3) and citrus (F2) isolates of HSVd. Top, primary structure. Differences are indicated by circles. Bottom, secondary structures of HSVd-Bor, -F3 and -F2 isolates showing various loops in the TR domain. Note differences in the number and size of the loops.

(VM) region (23, 30). Multiple alignment of the genome in this region indicated that HSVd-Bor and HSVd-F3 isolates have 100% homology while nucleotides 45 and 46 of HSVd-F2 isolate in PM and VM regions were absent. It has been assumed that pathogenicity is regulated by nucleotides within VM region (23). Thus deletion of nucleotides 45 and 46 in HSVd-F2 in this region may explain lower symptom severity of this isolate on greenhouse plants. Not many changes were observed in the CCR of these isolates. The only differences were related to the lower strand of HSVd-F2. HPI on upper strand in this region is a highly conserved structure in Pospiviroidae and

mediates cleavage and ligation of viroid concatomer. HPI consists of a tetra loop core and a highly conserved 3bp stem. Creation of mutation in conserved stem of HPI in PSTVd abolished the infectivity (22). Also mutation in tetra loop bases in PSTVd affected cleavage of concatomer compared to the wild type (22). Decrease in replication rate in HSVd-F2 with changes in lower CCR may be due to malfunction in viroid processing. According to the genomic map of viroid RNA motifs critical for replication and systemic trafficking described by Zhong *et al.* (22) HPI plays a role in viroid trafficking. The three isolates were completely similar in this region. This could

explain why they all caused systemic infection in greenhouse plants. In the V region of the genome, some differences were observed between these three isolates. The most remarkable difference was in G124, which is located on the last loop in the V region. Mutation in the last loop in the V domain of PSTVd reduced replication but the mutation was reverted to wild type showing the importance of this loop in biology of the viroid, although the exact function of this loop is not clear (22). Nucleotide change G124A was found in this loop of V domain in the HSVd-Bor genome. Therefore, given the importance of this loop in the viroid replication process, increasing the severity of symptoms of HSVd-Bor may be related to this change. Differences in the TR region have appeared in the form of substitutions and deletions. Structural determinants of systemic movement of the viroid are supposed to be in the TR domain (22, 30). All of these three isolates had systemic infection in host plants, so these differences did not affect systemic movement. In this study we found that HSVd-Bor isolate had a broader host range and more severe symptoms than the other two isolates. In PSTVd, severity of symptoms and symptom type are highly dependent on the concentration of the viroid generated siRNA in the tissues. Severe strains of PSTVd induced more siRNA than conventional strains (32, 33). Thus increase or decrease in symptom severity of different HSVd isolates may be the result of differing abilities of the isolates in siRNA production. It would be of interest to study siRNA content of biologically different HSVd isolates. Pathogenicity is a complex aspect of viroid biology. It seems that the disease is the result of interactions of different viroid domains as well as interaction of the latter with host factors (34). The role of RdR6 as a host factor in symptom development of PSTVd has been demonstrated (34). So this factor may also be determinative in the infectivity of HSVd isolates in host plant .

The present study points to the significance of various nucleotides and motifs in the infectivity of HSVd isolates. However, mutational analysis is needed to establish their

functional roles in the biology of the viroid. Also in this study apple, quince, apricot and peach were shown to be infected by HSVd for the first one in Iran. The significance of this finding needs further investigation.

## References

1. Diener TO. Subviral pathogens of plants: Viroids and viroidlike satellite RNAs. *FASEB J.* 1991;5:2808-13.
2. Hadidi A, Flores R, Randles J W, Semancik J S. "Viroids". CSIRO Publishing, Australia. 2003;370pp.
3. Shikata E. New viroids from Japan. *Sem Virol.* 1990;1:107-15.
4. Polivaka H, Staub U, Gross HJ. Variation of viroid profiles in individual grapevine plants: Novel grapevine yellow speckle viroid I mutants show alternations in hairpin. *J Gen Virol.* 1996;77:155-61.
5. Astruc N, Marcos JF, Macquaire G, Candresse T, Pallas V. Studies on the diagnosis of hop stunt viroid in fruit trees: Identification of new hosts and application of a nucleic acid extraction procedure based on nonorganic solvents. *European J. Plant Pathol.* 1996;102:837-46.
6. Sano T, Hataya T, Terai Y, Shikata E. Hop stunt viroid strains from dapple fruit disease of plum and peach in Japan. *J Gen Virol.* 1989;70:1311-9.
7. Diener T, Smith, Hammond R, Albanese G, La Rosa R, Davino M. Citrus B viroid identified as a strain of hop stunt viroid. *Plant Dis.* 1988;72:691-693.
8. Semancik J, Roistacher C, Rivera-Bustamante R, Duran-Vila N. Citrus cachexia viroid , a new viroid of citrus: Relationship to viroids of the exocortis disease complex. *J Gen Virol.* 1988;69:359-3068.
9. Hsu Y, Chen W, Owens RA. Nucleotide sequence of a hop stunt viroid variant isolated from citrus growing in Taiwan. *Virus Genes.* 1994;9:193-5.
10. Palacio-Bielsa A, Romero J, Duran-Vila N. 2004. Characterization of citrus HSVd isolates. *Arch Virol.* 2004;149:537-52.
11. Amiri Mazhar M, Bagherian SAA, Izadpanah K. 2013. Variants of hop stunt viroid associated with mulberry vein clearing in Iran. *J Phytopathol.* 2013;162:269-71.
12. Amiri Mazhar M, Bagherian SAA, Salahi Ardakani A, Izadpanah K. Nucleotide sequence and structural features of hop stunt viroid and citrus bent leaf viroid variants from blighted citrus plants



In Kohgiluyeh–Boyerahmad Province of Iran. *J Agr Sci Tech*. 2014;16:657-65.

13. Bagherian SAA, Izadpanah K. Two novel variants of hop stunt viroid associated with yellow corky vein disease of sweet orange and split bark disorder of sweet lime. 21st International Conference on Virus and other Graft Transmissible Diseases of Fruit Crops, Julius-Kühn-Archiv. 2010;427:105-13

14. Gambino G, Perrone I, Gribaudo I. A Rapid and effective method for RNA extraction from different tissues of grapevine and other woody plants. *Phytochem Anal*. 2008;19:520–5.

15. Serra P, Gago S, Duran-Vila N. A single nucleotide change in Hop stunt viroid modulates citrus cachexia symptoms. *Virus Res*. 2008;138:130–4.

16. Amari K, Gomez G, Myrta A, Di Terlizzi B, Pallas V. The molecular characterization of 16 new sequence variants of Hop stunt viroid reveals the existence of invariable regions and a conserved hammerhead-like structure on the viroid molecule. *J Gen Virol*. 2001;82:953–962.

17. Roistacher CN. The cachexia and xyloporosis diseases of citrus: A review. pp. 116-123, In Proc. 10th Conf IOCV, Riverside, CA. 1988.

18. Sano T. 2012. History, origin, and diversity of hop stunt and hop stunt viroid. III International Humulus Symposium, Book of Abstracts. 2012; 36.

19. Owens RA, Chen W, Hu Y, Hsu YH. Suppression of potato spindle tuber viroid replication and symptom expression by mutations which stabilize the pathogenicity domain. *Virology*. 1995;208:554–64.

20. Owens RA, Steger G, Hu Y, Fels A, Hammond RW, Riesner D. RNA structural features responsible for potato spindle tuber viroid pathogenicity. *Virology*. 1996;222:144–58.

21. Grunner R, Fels A, Qu F, Zimmat R, Steger G, Riesner D. Interdependence of pathogenicity and replicability with potato spindle tuber viroid. *Virology*. 1995;209:60-9.

22. Zhong X, Archual JA, Amin AA, Ding B. A genomic map of viroid RNA motifs critical for replication and systemic trafficking. *Plant Cell*. 2008;20:35-47 .

23. Schnolzer M, Hass B, Ramm K, Hofman H, Sanger HL. Correlation between structure and

pathogenicity of potato spindle tuber viroid (PSTVd). *EMBO J*. 1985;4:2181-90.

24. Keese P, Symons RH. Domains in viroids: Evidence of intermolecular RNA rearrangement and their contribution to viroid evolution. *Proc Natl Acad Sci USA*. 1985;82:4582-6.

25. Hammond RW. Analysis of the virulence modulating region of potato spindle tuber viroid (PSTVd) by site-directed mutagenesis. *Virology*. 1992;187:654-62.

26. Zaki-Aghl M, Izadpanah K, Niazi A, Behjatnia SAA, Afsharifar A. 2013. Molecular and biological characterization of the Iranian isolate of the Australian grapevine viroid. *J Agr Sci Tech*. 2013; 15: 855-865.

27. Owens RA, Hammond RW. Viroid pathogenicity: One process many faces. *Viruses*. 2009;1:298-316.

28. Ding B. The biology of viroid-host interactions, *Annu. Rev. Phytopathol*. 2009;47:105-31.

29. Flores R, Gas ME, Molina- Serrano D, Nohales MA, Carbonell A, Gago S, De la Pena, M, Daros JA. 2009. Viroid replication: Rolling-circles, enzymes and ribozymes. *Viruses*. 2009;1:317-34.

30. Steger G, Hofmann H, Foartsch J, Gross HJ, Randles JW, Sanger HL, Reisner D. Conformational transitions in viroids and virusoids: comparison of results from energy minimization algorithm and from experimental data. *J Biomol Struct Dyn*. 1984;2:543-71.

31. Takeda R, Ding B. Viroid intercellular trafficking: RNA motifs, cellular factors and broad impacts. *Viruses*. 2009;1:210- 21.

32. Vogt U, Pelissier T, Putz A, Razvi F, Fischer R, Wassenegger M. Viroid-induced RNA silencing of GFP viroid fusion transgenes does not induce extensive spreading of methylation or transitive silencing. *Plant J*. 2004;38:107–18.

33. Wang MB, Bian XY, Wu LM, Liu LX, Smith NA, Isenegger D, et al. On the role of RNA silencing in the pathogenicity and evolution of viroids and viral satellites, *Proc Natl Acad Sci USA*. 2004;101:3275-80.

34. Gomez G, Martinez G, Pallas V. Viroid-induced symptoms in *Nicotiana benthamiana* plants are dependent on RDR6 activity. *Plant Phys*. 2008;148:414–23.